Available online at www.sciencedirect.com
ScienceDirect
Journal of Hazardous Materials 144 (2007) 355–362
Journal of Hazardous Materials
www.elsevier.com/locate/jhazmat

Adsorption of a cationic dye (methylene blue) onto spent activated clay

Chih-Huang Weng *, Yi-Fong Pan

Department of Civil and Ecological Engineering, I-Shou University, Da-Hsu Township, Kaohsiung 84008, Taiwan

Received 8 June 2006; received in revised form 23 September 2006; accepted 25 September 2006
Available online 18 October 2006

Abstract

The adsorption characteristics of methylene blue (MB) onto spent activated clay (SAC), a waste produced from an edible oil manufacturer was investigated. Results showed that the adsorption increased with increasing MB concentration, temperature, and pH. The adsorption equilibrium data was well fitted by multilayer adsorption isotherm. The maximum adsorption capacities for MB ranged from 0.94×10^{-4} to 3.41×10^{-4} mol/g between 5 and 45 °C. Thermodynamic parameters suggest that the adsorption is spontaneous and endothermic. We proposed a modified double exponential equation accounting both with chemical and mathematical point of view to describe the adsorption kinetic data. The increases of mass transfer and adsorption capacity were mainly attributed to the interlayer of the SAC expanding at higher temperature. An activation energy of 13.5 kcal/K mol was determined suggesting that the adsorption involved a chemical reaction mechanism.

Keywords: Adsorption; Dye; Spent activated clay; Methylene blue

1. Introduction

Dyes are widely used in industries such as textiles, pulp mills, leather, dye synthesis, printing, food, and plastics, etc. Since many organic dyestuffs are harmful to human being and toxic to microorganisms, removal of dyestuffs from wastewater has received considerable attention over the past decades. Various treatment methods have been developed for decontamination purposes including coagulation, chemical oxidation, membrane separation, electrochemical process, and adsorption techniques. Of the above mentioned techniques, adsorption was recognized to be a promising and a cost-effective process to remove colors from aqueous solution. Many kinds of adsorbents have been developed for various applications [1–9]. Due to its effectiveness and versatility, activated carbon is widely employed in water and wastewater treatment. However, the operating cost of activated carbon adsorption is high. Problems of regeneration and difficulty in separation from the wastewater after use are the two major concerns of using this material. This has led to searches for unconventional adsorbents as alternative adsorbents. The use of unconventional adsorbent has the following features: (1) it can be obtained abundant locally and cheaply. Most of them are readily to be utilized; (2) regeneration of these low-cost substitutes is not necessary whereas regeneration of activated carbon is essential. Such regeneration may result in additional effluent and the adsorbent may suffer a considerable loss; (3) less operation cost in terms of maintenance and supervision are required for the unconventional adsorption systems; (4) utilization of industrial solid waste for the treatment of industrial wastewater is helpful not only to the environment, but also to reduce the disposal cost.

The activated clay is an expanding 2:1 layer silicate mineral, which mainly consists of montmorillonites. The specific surface area (SSA) of montmorillonite is about 31–61 m^2/g [10,11]. Once it was activated with sulfuric acid, the surface area of activated clay could increase up to 300 m^2/g. As such, the activated clay also known as bleaching earth is applied to the edible oil refinery industry to remove color substances and undesirable residues from crude oil. After the bleaching process, the refinery residue (spent activated clay (SAC)) was disposed directly into the landfill without considering regeneration. Because this waste contains about 20–40% (w/w) of residual oil that can oxidize to the point of spontaneous combustion [12], it presents a fire hazard to the landfill and produces unpleasant odors. In Taiwan the annual production of SAC is approximately 2310–5390 metric tonnes [13]. Realizing the beneficial uses of this industrial waste, Taiwan Environmental Protection Administration (EPA) has promulgated a resource conservation directive to reuse the oil processing waste as follows: (1) additives for cement, (2)

* Corresponding author. Tel.: +886 7 6578957; fax: +886 7 6577461.
E-mail address: chweng@isu.edu.tw (C.-H. Weng).

0304-3894/$ – see front matter © 2006 Elsevier B.V. All rights reserved.
doi:10.1016/j.jhazmat.2006.09.097

additives for oilseed dregs produced in the edible plant oil industry, (3) raw material for organic fertilizer, and (4) fuel [13]. Other than the above utilization, under proper treatment, this waste could turn into a useful product, such as (1) extracting the retaining oil for fuel substitute or animal feed; (2) reused as an adsorbent in wastewater treatment plants; (3) utilizing it as clay substitute in the brick and tile manufacturing process [14–17].

Based on the above viewpoints, a SAC sample generated from an edible oil refinery company in southern Taiwan was investigated for its potential use as adsorbent for the removal of dyestuff from aqueous solution. Despite the fact that the production of the SAC in this company alone is about 2500–3000 metric tonnes per year, utilization of this waste as an adsorbent has not yet been considered. Methylene blue (MB), a water-soluble cationic dye, was used as a target contaminant to characterize the adsorptive properties of this waste. Parameters affecting the adsorption including initial dye concentration, pH, and temperature were evaluated. Models to fit the adsorption equilibrium and kinetic data were presented. Results of this study will be useful for using this waste as an economic adsorbent in the removal of cationic dyes from wastewater.

2. Materials and methods

2.1. Spent activated clay

Fig. 1 shows the SEM micrograph of a typical SAC sample at 5000× magnification. The SAC particles were mostly irregular in shape and porous. A pH of 3.37 was obtained from immersing it in a solution containing 1:1 (v/v) ration of SAC and distilled water. The component of this activated clay is SiO_2 (65–75%), Al_2O_3 (15–20%), MgO (2.5%), Fe_2O_3 (2%), and CaO (0.5%). The color of fresh activated clay is white. Once it was used to remove the color from edible oil, the color of activated clay has changed from white to brownish. For the purposes of removing oil and other residues left in the SAC and to recover more activate adsorption site, the raw SAC sample was treated as follows: (1) mix 250 g SAC sample with 2 L distilled water; (2) place the solution in a high pressure cooker (S–328, First Lady, Taiwan) under a pressure of 10 psi at 100 °C for 15 min; (3) after cooking, remove the supernatant and rinsed the cooked SAC with distilled water; (4) run the process from step (1) to (3) for five times until the color of the supernatant turns white; (5) Oven-dried overnight and store in a desiccator; (6) measure the oil content of this treated SAC. This process can extract a large portion of oil from raw SAC. The oil content of treated SAC dropped from the original of 13.1 to 2.9%. The oil soxhlet extraction method was followed by the procedure describe in APHA [18]. The cation exchange capacity (CEC), BET-N_2 SSA, and average pore radius for the treated SAC are 55.7 cmol/kg, 10.1 m^2/g, and 6.84 nm, respectively. CEC was determined according to Taiwan EPA method NIEA S202.60A [19]. The BET-N_2 SSA and average pore radius of the SAC samples were determined by a surface area analyzer (Coulter SA3100, Beckman). The pH_{zpc} of the SAC particulates was 2.8 determined by a zeta potential meter (Laser Zee 3.0, Pen Kem Inc.).

Fig. 1. SEM image (5000×).

2.2. Dye

MB was purchased from Riedel-de Haën Co. (Germany). The formula is $C_{16}H_{18}N_3SCl{\cdot}3H_2O$ and the structural formula of the dye is given in Fig. 2. The aromatic moiety of MB contains N and S atoms. In the aromatic unit, dimethylamino groups attach to it. The aromatic moiety is planar and the molecule is positively charged.

2.3. Equilibrium adsorption experiments

The experimental procedures for the adsorption equilibrium as affected by solution pH were described as follows: (1) prepare a 1-L solution with a constant strength of $NaNO_3$ (5×10^{-2} M) and different MB concentrations; (2) distribute 100 mL of solution to a series of 125-mL polyethylene (PE) bottles; (3) adjust initial pH to cover a range from 2 to 10 by either HCl or NaOH; (4) add a given amount of air-dried SAC (0.2 g/L) into the solution; (5) shake these bottles on a reciprocal shaker at 150 excursions/min for 5 h at 25 °C. This contact time was found to be adequate for reaching equilibrium adsorption based on the results of kinetic study; (6) at the end of shaking, record the final pH of the mixed liquor; (7) filter the liquor through a 0.45-μm filter paper (supor-450, Gelman Sci.) to collect the supernatant; (8) determine the residual MB concentration in the supernatant. Blank tests without adsorbent (SAC) in the mixed suspension were also performed to avoid possible adsorption on the PE bottles and the filter apparatus used. The residual MB concentration in the supernatant was analyzed using a spectrophotometer

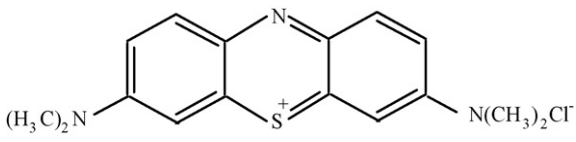

Fig. 2. Molecular structure of MB.

(HACH DR-2010, USA) at a wavelength of 615 nm. The effect of temperature on adsorption was investigated under isothermal conditions at 5, 15, 25, 30, 35, and 45 °C by maintaining the mixtures in a water circulation bath whose temperature varied within ±0.2 °C. The experimental procedures employed for studying the effect of temperature on the dye adsorption isotherm were the same as those described in the section above except that the pH of the mixed solution was adjusted to 5.5 in step (3) and the temperature was controlled in step (5).

Kinetic adsorption experiments were conducted to establish the effect of time on the adsorption process and to identify the adsorption rate. Factors affecting the adsorption rate including pH and temperature were performed. The general procedures for kinetic experiments are described as follows: (1) prepare 1 L solution containing a fixed MB concentration with a constant ionic strength of $NaNO_3$; (2) adjust solution pH to a desired value either with 0.1 M HCl or 0.1 M NaOH solution; (3) add a given amount of the air-dried SAC (0.2 g/L) into the solution; (3) agitate these solutions on a magnetic stirrer at 300 rpm for 5 h at room temperature (25 °C); (4) at the completion of preset time intervals, a 5 mL of solution was taken and immediately filtered through the 0.45 μm membrane filter to collect the supernatant; (5) determine the residual MB concentration in the supernatant. The effect of pH on adsorption rate was conducted by the same procedures described above except that in step (2) the pH of the solution was maintained at 3.0 ± 0.05, 5.5 ± 0.1, 7.5 ± 0.1, and 9.5 ± 0.05. The effect of temperature on adsorption rate was conducted under isothermal conditions at 15, 25, 30, 35, and 45 °C by maintaining the mixtures in a water circulation bath whose temperature varied within ±0.2 °C. In order to assume maintaining thermal equilibrium, the 1-L bottle was first placed into the temperature controlled bath for about 0.5 h prior to the experiments. Adsorption capacity of the SAC sample was calculated as follows:

$$q_t = \frac{C_0 - C_t}{w} \tag{1}$$

where q_t (mol/g) is the amount of MB adsorbed at contact time t (min), C_0 (mol/L) is the initial MB concentration, C_t is the MB concentration at time (t), and w (g/L) is the SAC amount in the solution. All experiments were replicated and the average values were used in the data analysis.

3. Model fitting

3.1. Isotherm models

A multilayer adsorption isotherm model was applied to fit the data [20]:

$$q = \frac{Q_m K_1 C_e}{(1 - K_2 C_e)[1 + (K_1 - K_2)C_e]} \tag{2}$$

where q is the amount of MB adsorbed at equilibrium; Q_m is the maximum monolayer adsorption density (original SAC site density, mol/g); C_e is the equilibrium MB concentration (mol/L); K_1 is the adsorption affinity constant for the first layer; K_2 represents the adsorption affinity for subsequent multilayer. If the value of K_2 is assumed to be negligible on the overall adsorption, Eq. (2) is reduced to the Langmuir isotherm equation:

$$q = \frac{Q_m K_1 C_e}{1 + K_1 C_e} \tag{3}$$

3.2. Kinetic models

A double exponential equation (DEE) accounting both with chemical and mathematical point of view was used to describe the adsorption kinetics of MB onto SAC. This model is based on a mathematical solution to describe a two-step mechanism [21]:

$$q_t = q_e - \frac{D_1}{w}\exp(-K_{D_1}t) - \frac{D_2}{w}\exp(-K_{D_2}t) \tag{4}$$

where q_e is the amount of MB adsorbed (mol/g) at equilibrium, D_1 and D_2 (mol/L) are the adsorption coefficients of the rapid and the slow steps, respectively, and K_{D_1} and K_{D_2} (1/min) are the mass transfer coefficients of the rapid and slow phase, respectively. The DEE can be considered as a diffusion model because K_{D_1} and K_{D_2} are the diffusion parameters controlling the overall kinetics. The rapid-step mass transfer coefficient, K_{D_1}, covers both external and internal diffusion while the slow-step K_{D_2} takes into account intraparticle diffusion. The external mass transfer, k_e (m/min), and internal mass transfer, k_i (m/min), can be calculated as follows [21]:

$$K_{D_1} = (k_e + k_i)S_e w\frac{C_0}{C_0 - C_{eq}} \tag{5}$$

$$K_{D_2} = k_i S_i w\frac{C_0}{C_0 - C_{eq}} \tag{6}$$

where S_e and S_i are the external and internal surface area (m^2/g), respectively, C_{eq} is the equilibrium solute concentration (mol/L). The DEE can be used to explain the adsorption process involved with two different adsorption sites. Fletcher et al. [22] used K_{D_1} and K_{D_2} as kinetic rate constants and used them to describe the adsorption of methanol and ethanol on organic porous structures. A graphical computer software, viz. KaleidaGraph™ [23], was used to solve the above kinetic and equilibrium equations.

4. Results and discussion

4.1. Equilibrium studies

4.1.1. Effect of pH on the adsorption equilibrium

The effect of solution pH on the amount of MB adsorbed was studied by varying initial pH under different MB concentrations at 25 °C. The results of percentage MB removal versus equilibrium pH are shown in Fig. 3. It was found that an increase initial MB concentration lead to a decrease in the MB removal efficiency. In other words, the percentage MB removed was inversely proportional to the surface loading (initial MB concentration divided by adsorbent concentration). A higher surface loading leads to a greater competition of MB ions themselves with a fixed surface adsorbing sites. Consequently, a less removal efficiency resulted. As shown, the removal efficiency of MB

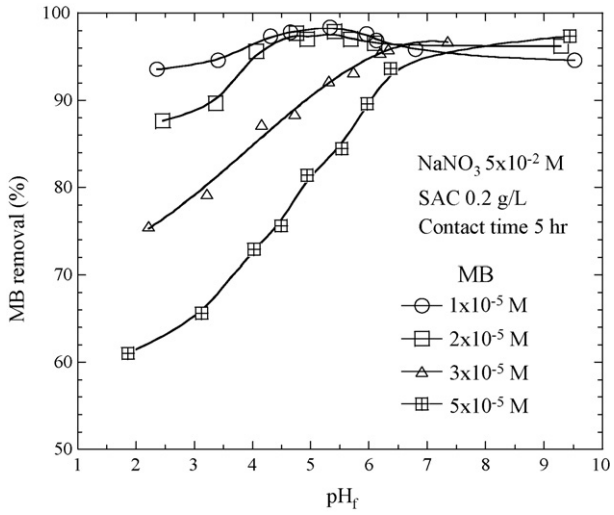

Fig. 3. Effect of pH on the removal of MB by spent activated clay. Experimental condition: SAC 0.2 g/L; $NaNO_3$ 5×10^{-2} M; contact time 5 h; 25 °C.

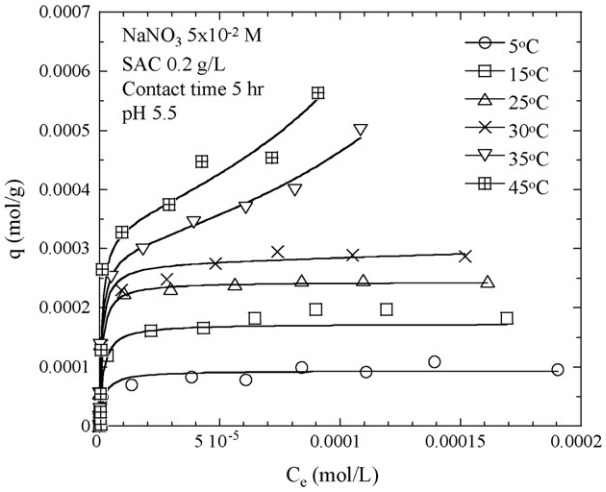

Fig. 4. Effect of temperature on the isotherm for MB adsorption onto spent activated clay. Solid lines are the best fit of multilayer model.

increased with increasing pH. An abrupt increases in the MB removal was found at pH range from 2.0 to 6.5. The extent of adsorption was observed to become nearly constant at pH values greater than 6.5. More than 95% removal was found over the pH ranges of 6.5–9.5. The solution pH appears to be a key factor affecting the adsorption characteristics of MB onto SAC. The strong dependence of adsorption on pH could be attributed to the fact that the surface charge of SAC was greatly affected by solution pH. Increasing solution pH resulted in an increasing surface potential allowing for the adsorption of the basic MB dye. When the solution pH is greater than the pH_{zpc}, the negative charged SAC surface is favorable for the adsorption MB dye. Since the edges of activated clay are identical to the surface of a mixture of oxides, it acts similar to those oxide surfaces providing affinity sites for MB adsorption. The degree of adsorption would be influenced by the development of pH-dependent charge on the edges (or so called layer charge) due to acid base reactions of surface groups. Thus, the pH dependent adsorption of MB onto SAC may be described as follows:

$$\underline{S}\text{–OH} + MB^+ = \underline{S}\text{–O–MB} + H^+ \quad (7a)$$

or

$$\underline{S}\text{–O}^- + MB^+ = \underline{S}\text{–O–MB} \quad (7b)$$

where S represents the active surface functional groups including the silanol (Si–O$^-$) and aluminol (Al–O$^-$) sites; S–OH and S–O$^-$ refer to neutral and ionized surface hydroxyl functional groups.

4.1.2. Adsorption isotherms

Fig. 4 shows the effect of temperature on the MB adsorption isotherms. As shown the amount of MB adsorbed increased with increasing temperature. The solid lines in Fig. 4 are the best fits of the multilayer model (Eq. (2)). The maximum monolayer adsorption density (Q_m) and the corresponding equilibrium constants (K_1 and K_2) are listed in Table 1. The high value of the correlation coefficient ($r^2 > 0.90$) indicates that the experimental data were well correlated by the multilayer model. It is visualized that the isotherms exhibited two identical adsorption characteristics. A monolayer type of isotherm was found for the experiments of 5, 15, 25 °C and a multilayer type for above 30 °C. As shown in Table 1, the values of Q_m are 9.4×10^{-5}, 1.73×10^{-4}, 2.44×10^{-4}, 2.77×10^{-4}, 2.98×10^{-4}, and 3.41×10^{-4} mol/g, respectively, for 5, 15, 25, 30, 35, and 45 °C. It is speculated that the interlayer of the SAC were enlarged allowing more MB adsorption under a higher temperature condition. For the experiments above 30 °C, the K_2 values remain relatively constant suggesting the multilayer adsorption was not greatly affected by changes in the temperature. The K_1 values (5.46×10^5–9.89×10^5 L/mol) were indeed much greater than those of K_2 (361–4272 L/mol), indicating that the adsorption affinity of the first layer was much higher than that of the subsequent multilayer. The results revealed that the magni-

Table 1
Isotherm fitting constants for the adsorption of MB onto SAC

	Temperature (°C)					
	5	15	25	30	35	45
Q_m (mol/g)	0.94×10^{-4}	1.73×10^{-4}	2.44×10^{-4}	2.77×10^{-4}	2.98×10^{-4}	3.41×10^{-4}
K_1	5.46×10^5	6.48×10^5	9.39×10^5	9.45×10^5	9.68×10^5	9.89×10^5
K_2	0	0	0	361	3620	4272
r^2	0.931	0.964	0.941	0.959	0.970	0.900

Table 2
Comparison of adsorption capacity of methylene blue on various adsorbents

Adsorbent	SSA (m^2/g)	pH	Temperature (°C)	Q_m (mol/g)	K (L/mol)	References
Clay minerals						
SAC	10.1	5.5	25	2.44×10^{-4}	9.39×10^{5}	This study
Clay	30	NA	20	1.98×10^{-5}	2.49×10^{2}	[24]
Bentonite	NA	NA	25	3.80×10^{-4}	2.10×10^{6}	[25]
Thermal-bentonite	NA	9	25	4.61×10^{-5}	1.53×10^{5}	[26]
SDS-bentonite	NA	9	25	4.26×10^{-5}	3.96×10^{5}	[26]
Waste materials						
Sludge	493.6	NA	25	2.29×10^{-4}	5.55×10^{5}	[27]
Orange peel	22.1	7.2	30	5.51×10^{-5}	6.72×10^{6}	[28]
Fly ash	6.52	8	30	1.49×10^{-5}	2.02×10^{5}	[29]
Sludge ash	3.7	9.8	24	5.00×10^{-6}	4.29×10^{5}	[4]
Coal fly ash	5.47	NA	22	3.60×10^{-6}	1.47×10^{5}	[30]
Lignite coal	7.6	NA	20	1.20×10^{-7}	2.85×10^{7}	[31]

Note: NA means not available. K is the Langmuir adsorption constant. Specific surface area was all determined by BET-N_2 method.

tude of adsorption increased with increasing the solution temperature, suggesting that the adsorption reaction was endothermic in nature. A comparison of MB adsorption capacities of various adsorbents is given in Table 2. It is seen that our results (2.44×10^{-4} mol/g) are quite similar to the investigations of sludge (2.29×10^{-4} mol/g) and bentonite (3.80×10^{-4} mol/g). The MB adsorption capacity and the adsorption affinity constants of SAC are much higher than other low-cost adsorbents such as fly ash, lignite coal, and orange peel. Variation in MB adsorption capacity and affinity is mainly attributed to the differences in experimental condition conducted and properties of adsorbent such as specific surface area.

The following thermodynamic parameters for the present system were determined, including the variation of free energy (ΔG°), enthalpy (ΔH°), and entropy (ΔS°):

$$\Delta G^\circ = -\mathrm{RT}\ \ln\ K \tag{8}$$

$$\ln\ K = \frac{\Delta S^\circ}{R} - \frac{\Delta H^\circ}{R}\frac{1}{T} \tag{9}$$

where R is the universal gas constant (1.987 cal/mol K); T is the absolute temperature (K); K is the equilibrium constant (L/mol). The values of ΔH° and ΔS° were determined from the slopes and intercept, respectively, from the van' Hoff plots. The calculated thermodynamic parameters based on the above functions are listed in Table 3. Because all ΔG° values are negative, it suggests that the adsorption process is spontaneous with high preference of MB for SAC. As shown, the magnitude of free energy for first layer adsorption (ΔG_1°) is much higher than that of the subsequent multilayer (ΔG_2°). For the multilayer adsorption, dye adsorption within the multilayer was attributed to the attachment of dye to the surface and to the subsequent layer. Thus, not only the adsorption affinity has a same order of magnitude, but also the adsorption energy would be much smaller than the monolayer. Generally, the value of ΔG° for physical adsorption is less than −4.7 kcal/mol while chemisorption is in the range of −19 through 95 kcal/mol [32]. As shown in Table 3, the values of ΔG_1° for the monolayer adsorption are in the middle of physical adsorption and chemisorption. For the multilayer adsorption with ΔG_2° ranging from −4.94 to −5.16 kcal/mol suggest that the adsorption process is a typical physical process. The values of ΔH_1° (2.91 kcal/mol) and ΔS_1° (36.8 cal/mol K) are positive, suggesting that the adsorption is spontaneous and endothermic.

4.2. Kinetic studies

4.2.1. Effects of pH

Fig. 5 shows the amount of MB adsorbed on SAC with time under different solution pHs. The solid lines represent the best fit of Eq. (4) to the experimental data. Table 4 lists the corresponding model fitting parameters, i.e. D_1, D_2, K_{D_1}, and K_{D_2}. The high r^2 (all >0.96) indicated that the data was well correlated to the DEE model. It is of interested to note that the fitting parameter for the rapid-step and slow-step are equal. As stated previously, the DEE may also be used to describe the adsorption of two different sites. In our case, since the parameters D_1 and D_2 are equal and K_{D_1} and K_{D_2} are also equal, it is suggested that the process is involved with one adsorption site. A modified DEE is expressed as:

$$q_t = q_e - \frac{D_T}{w}\exp(-K_D t) \tag{10}$$

Table 3
Thermodynamic parameters for the adsorption of MB onto SAC

	ΔG_1° at temperature (kcal/mol)						ΔH_1° (kcal/mol)	ΔS_1° (cal/mol K)
	5 °C	15 °C	25 °C	30 °C	35 °C	45 °C		
First layer	−7.32	−7.59	−8.14	−8.28	−8.44	−8.72	2.91	36.8
Multilayer	–	–	–	−3.55	−4.94	−5.16	–	–

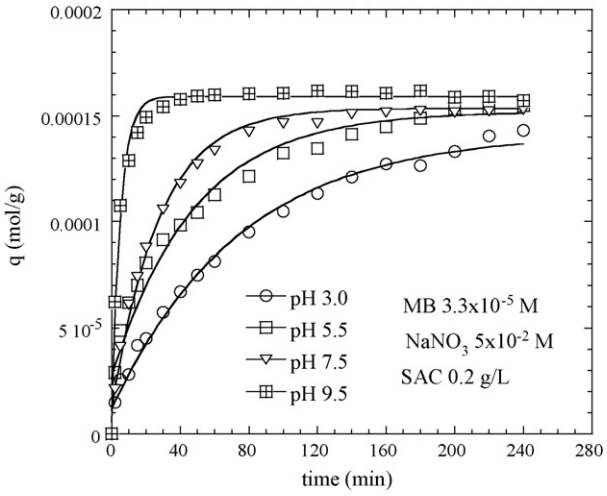

Fig. 5. Effects of pH on the adsorption kinetics of MB onto spent activated clay. Solid lines represent the best fit of double exponential equation.

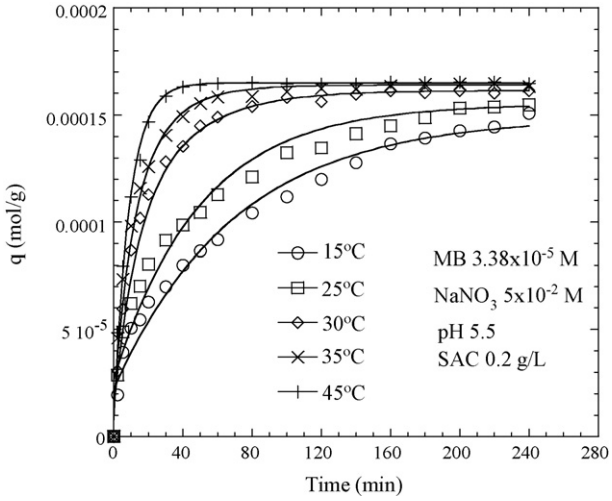

Fig. 6. Effects of temperature on the adsorption kinetics of MB onto spent activated clay. Experimental conditions: SAC 0.2 g/L; pH 5.5; MB 3.38×10^{-5} M; 25 °C. Solid lines represent the best fit of double exponential equation.

where K_D is the mass transfer coefficient, D_T is the overall adsorption coefficient which equals to $2D_1$ or $2D_2$. Values of D_T and K_D are listed in Table 4. These values indicated that increased pH could increase the mass transfer and the sorption affinity.

Considering only one active site taking place during adsorption, the external mass transfer, k_e, and the internal mass transfer, k_i, will be equal. In addition to that, only one apparent specific surface area of S_T (m^2/g) is considered. Thus Eqs. (5) and (6) yield:

$$K_{DT} = kS_T w \frac{C_0}{C_0 - C_{eq}} \tag{11}$$

where k is the overall mass transfer. Values of K_{DT} were listed in Table 5. Values of w and C_0 are 0.2 g/L and 3.3×10^{-5} M, respectively. S_T is 10.1 (m^2/g) as determined by BET-N_2 method. Based on Eq. (11), value of k was obtained (Table 4) for pH 5.5 at 25 °C. Results show that the mass transfer increased with increasing solution pH. By derivation of Eq. (10), the overall rate constants, r_T, become:

$$r_T = \frac{dq_t}{dt} = \frac{D_T}{w} K_{DT} \exp(-K_{DT} t) \tag{12}$$

At $t = 0$, the overall initial rate r_{To} (mol/min g) can be determined:

$$r_{To} = \frac{D_T}{w} K_{DT} \tag{13}$$

The obtained values of r_{To} are listed in Table 4. These results can be used to interpret with respect to the adsorption mechanism that is strongly affected by the solution pH. It is further confirmed that the adsorption rate increases with increasing solution pH.

4.2.2. *Effects of temperature*

The effect of temperature on the adsorption kinetics was investigated under isothermal conditions in the temperature range of 15–45 °C. The temperature dependence of MB adsorption kinetics is shown in Fig. 6. The experimental results indicate that the magnitude of adsorption is proportional to the solution

Table 4
Fitting parameters for DEE and modified DEE at various pHs

	pH			
	3.0	5.5	7.5	9.5
q_e (mol/g)	1.42×10^{-4}	1.52×10^{-4}	1.535×10^{-4}	1.595×10^{-4}
C_{eq} (mol/L)	4.6×10^{-6}	2.6×10^{-6}	2.3×10^{-6}	1.1×10^{-6}
Fitting parameters for DEE				
D_1 (mol/L)	1.304×10^{-5}	1.278×10^{-5}	1.417×10^{-5}	1.537×10^{-5}
K_{D_1} (1/min)	0.0134	0.0201	0.0377	0.1922
D_2 (mol/L)	1.304×10^{-5}	1.278×10^{-5}	1.417×10^{-5}	1.537×10^{-5}
K_{D_2} (1/min)	0.0134	0.0200	0.0377	0.1924
r^2	0.991	0.960	0.994	0.988
Fitting parameters for modified DEE				
D_T (mol/L)	2.608×10^{-5}	2.556×10^{-5}	2.834×10^{-5}	3.074×10^{-5}
K_{DT} (1/min)	0.0134	0.0201	0.0377	0.1922
k (m/min)	5.70×10^{-3}	9.16×10^{-3}	1.74×10^{-2}	9.20×10^{-2}
r_{To} (mol/min g)	1.69×10^{-6}	2.56×10^{-6}	5.40×10^{-6}	2.96×10^{-5}

Table 5
Fitting parameters for modified DEE at various temperatures

	Temperature (°C)				
	15	25	30	35	45
q_e (mol/g)	1.49×10^{-4}	1.52×10^{-4}	1.613×10^{-4}	1.639×10^{-4}	1.65×10^{-4}
C_{eq} (mol/L)	4×10^{-6}	2.6×10^{-6}	1.54×10^{-6}	1.02×10^{-6}	8×10^{-7}
Fitting parameters for DEE					
D_1 (mol/L)	1.266×10^{-5}	1.278×10^{-5}	1.480×10^{-5}	1.486×10^{-5}	1.571×10^{-5}
K_{D_1} (min^{-1})	0.0147	0.0201	0.0291	0.0464	0.1117
D_2 (mol/L)	1.266×10^{-5}	1.278×10^{-5}	1.480×10^{-5}	1.486×10^{-5}	1.571×10^{-5}
K_{D_2} (min^{-1})	0.0137	0.0200	0.0833	0.1049	0.1113
r^2	0.971	0.960	0.985	0.985	0.995
Fitting parameters for modified DEE					
D_T (mol/L)	2.532×10^{-5}	2.556×10^{-5}	2.96×10^{-5}	2.972×10^{-5}	3.142×10^{-5}
K_{DT} (1/min)	0.0095	0.02001	0.0290	0.0420	0.0882
k (m/min)	4.16×10^{-3}	9.16×10^{-3}	1.37×10^{-2}	2.02×10^{-2}	4.26×10^{-2}
r_{To} (mol/min g)	1.798×10^{-6}	2.560×10^{-6}	8.318×10^{-6}	1.124×10^{-5}	1.752×10^{-5}

temperature. Results show the amount of MB adsorbed increased from 1.49×10^{-4} to 1.65×10^{-4} mol/g when the temperature increased from 15 to 45 °C. The results of DEE model fitting shows the experimental data were well correlated with DEE model ($r^2 > 0.96$) (Table 5). As shown in Table 5, the magnitude of K_{D_1} and K_{D_2} values indicates that temperature plays an important role affecting the mass transfer in the adsorption process. Both K_{D_1} and K_{D_2} increased with the rise of temperature. It is speculated that the interlayer of SAC was enlarged under a higher temperature condition, therefore increasing its mass transfer of MB onto SAC.

In Table 5, it can be seen that the value of D_1 and D_2 are all equal for different temperatures. Theses results give us more confidence in the hypothesis of the one-site adsorption mechanism. Hence, the overall adsorption coefficient, D_T is used (Table 5) to account the sum of D_1 and D_2. The adsorption process apparently speeds up as the temperature increases. The value of K_D in Eq. (10) is related to the temperature:

$$K_{DT} = K_{25}(\theta)^{T-25} \tag{14}$$

where T is the temperature (°C), K_{DT} (1/min) is the mass transfer constant at T, K_{25} is the mass transfer constant determined at 25 °C (1/min), and θ is the temperature coefficient. The MB molecular diameter is 0.941 nm based on the value of apparent area 69.6 Å^2 [4]. Because the montmorillonite has an expandable interlayer spacing of 1.314 nm, the MB molecule should be able to enter the interlayer. As mentioned before, the interlayer spacing enlarged at a higher temperature and shrunk at a lower temperature. Therefore, the temperature coefficient can be treated as an expanding coefficient for the expandable interlayer of SAC. A value of θ 1.078 for temperature between 15 and 45 °C was determined on the basis of K_{D_1} and K_{D_2} values listed in Table 5. According to Eq. (14), the values of K_{DT} were determined (Table 5). As shown, a marked increase in K_{DT} occurs as temperature increased from 25 to 45 °C while it decreased as the temperature lowered to 15 °C.

The activation energy of the adsorption process, E, was calculated using the Arrhenius equation:

$$\ln(K_{DT}) = \ln(A) - \frac{E}{RT} \tag{15}$$

where A is referred to as the Arrhenius factor; R is the universal gas constant (1.987 cal/mol K); T is the absolute temperature (K). The rate constant K_{DT} listed in Table 5 was applied to estimate the activation energy of the adsorption. A value of 13.5 kcal/mol for E was obtained from the slope of an $\ln(K_{DT})$ versus $1/T$ plot with a r^2 of 0.999. Because the value of E is high, it is concluded that the adsorption kinetic of MB onto SAC involved a chemical reaction in the adsorption process.

5. Conclusions

The adsorption of MB onto spent activated clay is favored at high pH and higher temperature. The removal of methylene blue by adsorption on spent activated clay was found to be rapid at the initial period of contact time and then slows down with increasing reaction time. A modified double exponential equation (DEE) accounting both with chemical and mathematical point of view was used to describe the adsorption kinetics of MB onto SAC. We have developed a one-site adsorption process on the basis of the DEE model to fit the kinetic data. Results show that the mass transfer rate speeds up with increasing solution pH and temperature. The interlayer of the SAC sample expanded with increasing temperature and resulted in an increase of mass transfer and adsorption capacity. An activation energy of 13.5 kcal/K mol was determined suggesting that the adsorption involved a chemical reaction mechanism. A non-linear multilayer adsorption isotherm was used to describe the equilibrium adsorption isotherms. Results show that the isotherm exhibits a monolayer type of adsorption below 30 °C while it behaves as a multilayer at temperature above 30 °C. Thermodynamic parameters suggest that the adsorption is spontaneous and endothermic. This study showed that the SAC could be used as an adsorbent to remove MB dye from aqueous

solution. The SAC treated with a high pressure process has a maximum adsorption capacity of 2.44×10^{-4} mol/g at pH 5.5 and 25 °C. It is expected that a greater MB adsorption capacity would be resulted under an alkaline condition. Results of this study will be useful for future scale up using this waste material as a low-cost adsorbent for the removal of cationic dyes.

Acknowledgment

The work was supported by National Science Council of Republic of China (Grand No. NSC 94-2211-E-214-001).

References

[1] S. Wang, H. Lee, Dye adsorption on unburned carbon: kinetics and equilibrium, J. Hazard. Mater. B 126 (2005) 71–77.
[2] K.G. Bhattacharyya, A. Sharma, Kinetics and thermodynamics of methylene blue adsorption on neem (*Azadirachta indica*) leaf powder, Dyes Pigm. 65 (2005) 51–59.
[3] O. Hamdaoui, Batch study of liquid-phase adsorption of methylene blue using cedar sawdust and crushed brick, J. Hazard. Mater. B 135 (2006) 264–273.
[4] C.H. Weng, Y.F. Pan, Adsorption characteristics of methylene blue from aqueous solution by sludge ash, Colloids Surf. A: Physicochem. Eng. Aspects 274 (2006) 154–162.
[5] V.K. Gupta, D. Mohan, V.K. Saini, Studies on interaction of some azo dyes (naphthol red-J and direct orange) with nontronite mineral, J. Colloid Interf. Sci. 298 (2006) 79–86.
[6] V.K. Gupta, I. Ali, Suhas, D. Mohan, Equilibrium uptake and sorption dynamics for the removal of a basic dye (basic red) using low cost adsorbents, J. Colloid Interf. Sci. 265 (2003) 257–264.
[7] K.P. Singh, D. Mohan, G.S. Tandon, D. Gosh, Color removal from wastewater using low cost activated carbon derived from agricultural waste material, Ind. Eng. Chem. Res. (ACS) 42 (2003) 1965–1976.
[8] D. Mohan, K.P. Singh, G. Singh, K. Kumar, Removal of dyes from wastewater using fly ash—a low cost adsorbent, Ind. Eng. Chem. Res. (ACS) 41 (2002) 3688–3695.
[9] V.K. Gupta, D. Mohan, S. Sharma, M. Sharma, Removal of basic dyes (rhodamine-B and methylene blue) from aqueous solutions using bagasse fly ash, Sep. Sci. Tech. 35 (2000) 2097–2113.
[10] H. Green-Pedersen, N. Pind, Preparation, characterization, and sorption properties for Ni(II) of iron oxyhydroxide-montmorillonite, Colloids Surf. A: Physicochem. Eng. Aspects 168 (2000) 133–145.
[11] C. Pesquera, F. Gonzalez, I. Benito, S. Mendioroz, J.A. Pajares, Synthesis and characterization of pillared montmorillonite catalysts, Appl. Catal. 69 (1991) 97–104.
[12] S.J.T. Pollard, C.J. Sollars, R. Perry, The reuse of spent bleaching earth: a feasibility study in waste minimisation for the edible oil industry, Bioresource Technol. 45 (1993) 53–58.
[13] W.T. Tsai, Y.H. Chou, Government policies for encouraging industrial waste reuse and pollution prevention in Taiwan, J. Cleaner Prod. 12 (2004) 725–736.
[14] M. Daido, A recovery and reuse system for fatty oils from by-product and waste materials of vegetable fatty oil production, Conserv. Recycling 10 (1987) 273–278.
[15] Z. Werner, F.L. Prado, Safety & environment, Int. News Fats Oils Relat. Mater. 5 (1994) 1375–1383.
[16] W.T. Tsai, H.P. Chen, W.Y. Hsieh, C.W. Lai, M.S. Lee, Thermochemical regeneration of bleaching earth waste with zinc chloride, Resour. Conserv. Recycling 39 (2003) 65–77.
[17] W.T. Tsai, Y.M. Chen, C.W. Lai, C.C. Lo, Adsorption of ethyl violet dye in aqueous solution by regenerated spent bleaching earth, J. Colloid Interf. Sci. 289 (2005) 333–338.
[18] American Public Health Association (APHA), Standard Methods for the Examination of Water and Wastewater, Method 503C, 21st ed., American Public Health Association (APHA), 2005.
[19] Taiwan EPA (Environmental Protection Administration), Cation exchange capacity of soils (sodium acetate), Method NIEA S202.60A (1994).
[20] J. Wang, C.P. Huang, H.E. Allen, D.K. Cha, D.W. Kim, Adsorption characteristics of dye onto sludge particulates, J. Colloid Interf. Sci. 208 (1998) 518–528.
[21] P. Michard, E. Guibal, T. Vincent, C.P. Le, Sorption and desorption of uranyl ions by silica gel: pH, particle size and porosity effects, Micropor. Mater. 5 (1996) 309–324.
[22] A.J. Fletcher, E.J. Cussen, D. Bradshaw, M.J. Rosseinsky, K.M. Thomas, Adsorption of gases and vapors on nanoporous Ni_2(4,4′-bipyridine)$_3(NO_3)_4$ metal-organic framework materials templated with methanol and ethanol: structural effects in adsorption kinetics, J. Am. Chem. Soc. 126 (2004) 9750–9759.
[23] KaleidaGraph™ (Version 3.6), Synergy Software, Reading, PA, USA, 2003.
[24] A. Gurses, S. Karaca, C. Dogar, R. Bayrak, M. Acikyildiz, M. Yalcin, Determination of adsorptive properties of clay/water system: methylene blue sorption, J. Colloid Interf. Sci. 269 (2004) 310–314.
[25] C. Bilgic, Investigation of the factors affecting organic cation adsorption on some silicate minerals, J. Colloid Interf. Sci. 281 (2005) 33–38.
[26] S.A. Asheh, F. Banat, L.A. Aitah, The removal of methylene blue dye from aqueous solutions using activated and non-activated bentonites, Adsorp. Sci. Technol. 21 (2003) 451–462.
[27] N. Graham, X.G. Chen, S. Jayaseelan, The potential application of activated carbon from sewage sludge to organic dyes removal, Wat. Sci. Tech. 43 (2001) 245–252.
[28] G. Annadurai, R.L. Juang, D.J. Lee, Use of cellulose-based wastes for sorption of dyes from aqueous solutions, J. Hazard. Mater. 92 (2002) 263–274.
[29] K.V. Kumar, V. Ramamurthi, S. Sivanesan, Modeling the mechanism involved during the sorption of methylene blue onto fly ash, J. Colloid Interf. Sci. 284 (2005) 14–21.
[30] P. Janos, H. Buchtova, M. Ryznarova, Sorption of dyes from aqueous solutions onto fly ash, Water Res. 37 (2003) 4938–4944.
[31] S. Karaca, A. Gurses, R. Bayrak, Investigation of applicability of the various adsorption models of methylene blue adsorption onto lignite/water interface, Energy Convers. Manage. 46 (2005) 33–46.
[32] M.J. Jaycock, G.D. Parfitt, Chemistry of Interfaces, Ellis Horwood Limited, 1981.